Demarcating Curves for Shape Illustration

Michael Kolomenkin* Technion
Ilan Shimshoni† University of Haifa
Ayellet Tal‡ Technion

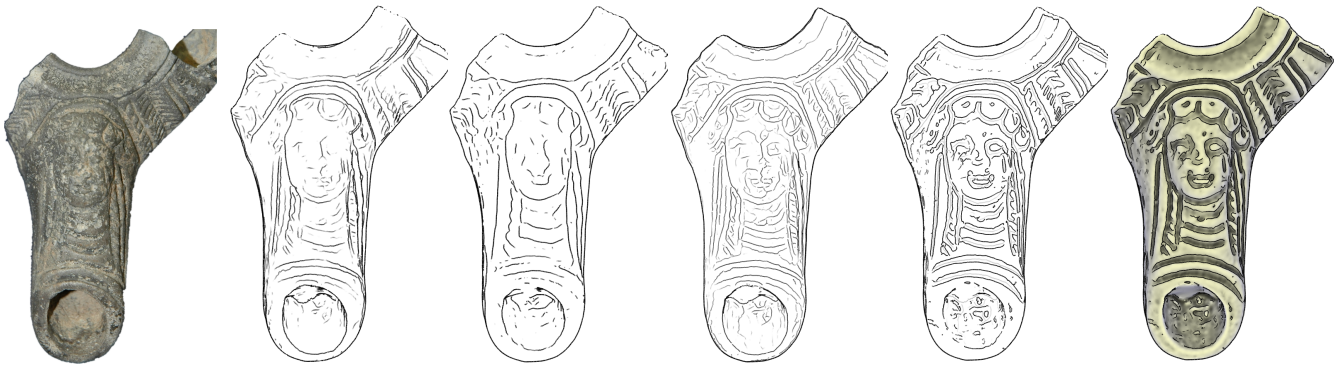

Figure 1: A late Hellenistic lamp (150-50 BCE) rendered with different feature curves

Abstract

Curves on objects can convey the inherent features of the shape. This paper defines a new class of view-independent curves, denoted *demarcating curves*. In a nutshell, demarcating curves are the loci of the "strongest" inflections on the surface. Due to their appealing capabilities to extract and emphasize 3D textures, they are applied to artifact illustration in archaeology, where they can serve as a worthy alternative to the expensive, time-consuming, and biased manual depiction currently used.

1 Introduction

Curves drawn on objects convey prominent and meaningful information about the shape. They can therefore be utilized in a large spectrum of applications, including non-photorealistic rendering [Strothotte and Schlechtweg 2002], segmentation [Stylianou and Farin 2004], robot navigation [Page et al. 2006], simplification [Pauly et al. 2003], brain analysis [Bartesaghi and Sapiro 2001], registration of anatomical structures [Pennec et al. 2000], and the recovery of archaeological and architectural information [Maaten et al. 2006]. Recent user studies [Cole et al. 2008] do not conclusively choose one of the current types of curves as the best for all cases. Therefore, the search for additional curves continues. Moreover, this search could be guided by specific application areas, where certain types of curves are preferred.

Feature curves can be classified as *view-dependent* or *view-independent* curves. View-dependent curves depend not only on the differential geometric properties of the surface, but also on the viewing direction. They change whenever the camera changes its position or orientation [Koenderink 1984; DeCarlo et al. 2003; DeCarlo and Rusinkiewicz 2007; Judd et al. 2007]. View-independent curves do not change with respect to the viewing direction [Interrante et al. 1995; Kalnins et al. 2002; Ohtake et al. 2004; Pauly et al. 2003; Yoshizawa et al. 2005]. One criticism of view-independent curves is that they can appear as markings on the surface [DeCarlo et al. 2003]. Even so, we believe there is merit to using such curves, in particular for applications such as archeology, architecture and medicine. We support this idea with a small study on artifact illustration in archeology.

This paper defines a new class of view-independent curves, termed *demarcating curves*. They are the loci of points for which there is a zero crossing of the curvature in the curvature gradient direction. Demarcating curves can be viewed as the curves that typically separate valleys and ridges on 3D objects (hence the name *demarcating*).

Our results demonstrate that demarcating curves effectively manage to capture 3D shape information visually. For instance, Figure 1 demonstrates its ability to depict the 3D texture of an object, such as the facial features and the hair, when comparing it to other well-known curves. They are as quick to compute as ridges and valleys and suggestive contours. Moreover, they can be combined with a shading model to jointly convey the details of the shape.

Archaeology has attracted a lot of attention of researchers in computer graphics and visualization [Rushmeier 2005; Koller et al. 2006; Brown et al. 2008]. This paper focuses on one aspect of archaeological research – relic illustration. Traditionally, archaeological artifacts are drawn by hand and printed in the reports of archaeological excavations – an extremely expensive and time-consuming procedure (e.g., Figure 2, [Stern 1995]). The main purpose of these drawings is to depict the features of the 3D object so that the archaeologist can visualize and compare artifacts without actually holding them in her hand. Such drawings are often inaccurate, since

*e-mail: michkol@tx.technion.ac.il
†e-mail: ishimshoni@mis.haifa.ac.il
‡e-mail: ayellet@ee.technion.ac.il

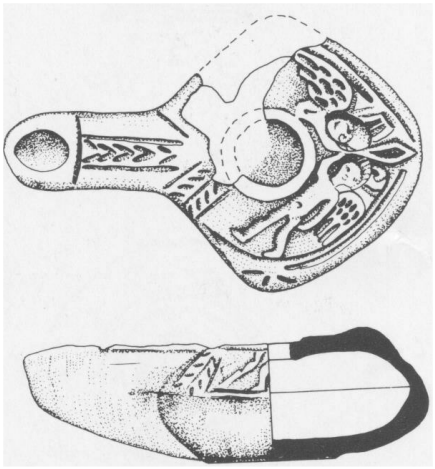

Figure 2: Lamp drawing in archaeology [Stern 1995]

the precision of the drawn curves depends on the qualifications of the artist. In addition, this technique does not always suffice due to space limitations that force the archaeologist to choose which objects will be drawn and decide on a small fixed set of viewing directions. Digitizing the findings by a high resolution scanner and drawing the curves directly on the scanned objects is a welcome alternative. This enables the archaeologist to study the artifact from all directions, with the 3D features highlighted.

The contribution of this paper is threefold. First, the paper presents demarcating curves, a new class of non-photorealistic view-independent curves on meshes. Second, some relationships of these curves to other well-known families of curves are discussed. Last but not least, these curves are applied to a real application – artifact illustration in archaeology. A preliminary user study indicates that archaeologists prefer for this purpose using demarcating curves to other types of curves or to manual drawing.

The paper is structured as follows. Section 2 reviews related work. Section 3 defines demarcating curves and describes the algorithm for computing them. Section 4 discusses relations of demarcating curves to other curves. Section 5 presents some results. Section 6 discusses the use of the curves for artifact illustration in archaeology. Section 7 concludes the paper.

2 Related work

The approaches for drawing curves characterizing objects in 3D can be categorized according to whether they depend on the viewpoint. A variety of view-dependent curves has been proposed. *Contours (silhouettes)*, which represent the "object outline," are the loci of points at which the object normal is perpendicular to the viewing direction [Koenderink 1984; Gooch et al. 1999; Hertzmann and Zorin 2000]. *Suggestive contours* are the loci of points at which occluding contours appear with minimal change in viewpoint [DeCarlo et al. 2003; DeCarlo et al. 2004]. They correspond to true contours at nearby viewpoints. *Highlight lines* extend the suggestive contours [DeCarlo and Rusinkiewicz 2007]. They roughly correspond to ridges of intensity in diffuse-shaded images. *Apparent ridges* are defined as the ridges of view dependent curvature [Judd et al. 2007]. *Photic extremum lines* are the set of points where the variation of illumination in the direction of its gradient reaches a local maximum [Xie et al. 2007].

Other view-dependant approaches utilize image edge detection algorithms by drawing the curves on the projections of the objects to the image [Lee et al. 2007; Pearson and Robinson 1985; Iverson and Zucker 1995; Saito and Takahashi 1990]. These approaches assist in correct scale selection and may reduce the computational complexity. However, pixel-based representation of image edges might yield low precision. View-dependent curves look visually pleasing and hence suit non-photorealistic rendering applications.

There are a number of view-independent curves. The most common curves are *ridges and valleys* [Interrante et al. 1995; Kalnins et al. 2002; Ohtake et al. 2004; Pauly et al. 2003; Yoshizawa et al. 2005], which occur at points of extremal principal curvature. Ridges and valleys portray important object properties. However, drawing only valleys (or ridges) is often insufficient, since they do not always convey the structure of the object. Drawing both will overload the image with too many lines. Moreover, coloring these lines so as to differentiate between them might be cumbersome [Interrante et al. 1995]. Other view-independent curves are *parabolic lines*, which partition the surface into hyperbolic and elliptic regions, and *zero-mean curvature curves*, which classify sub-surfaces into concave and convex shapes [Koenderink 1990].

3 Demarcating curves

Given a surface in 3D, we can imagine it locally as a terrain with ridges and valleys. Intuitively, *demarcating curves* run on the slopes between the ridges and the valleys. Figure 3 shows an example of such a local terrain, where the magenta cross section transverses from concave (valley) to convex (ridge) and the demarcating curve point (green) is the transition point. In other words, demarcating curves are the loci of the "strongest" *inflections* on the surface (i.e., where the transition from convex to concave is the fastest). The challenge is to find them. Below, we define this notion formally.

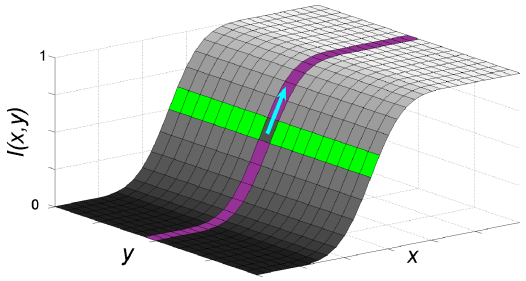

Figure 3: Local terrain (smoothed step edge); the demarcating curve in green; the cross section orthogonal to it in magenta; its local direction $\mathbf{g}_p$ in cyan.

3.1 Defining demarcating curves

Before defining the curves, we review the definitions of the normal section, normal curvature, the second fundamental form, and the derivatives of curvature [Do Carmo 1976]. The motivation for using these quantities is that they are intrinsic properties of the surface and are therefore invariant to rigid transformations.

The *normal section* of a regular surface at point $\mathbf{p}$ in tangent direction $\mathbf{v}$ is the intersection of the surface with the plane defined by the normal to the surface at $\mathbf{p}$ and $\mathbf{v}$.

The *normal curvature* at point $\mathbf{p}$ in direction $\mathbf{v}$ is the curvature of the normal section at $\mathbf{p}$, where the curvature of a curve is the reciprocal of the radius of the circle that best approximates the curve at $\mathbf{p}$.

For a smooth surface, the normal curvature in direction $\mathbf{v}$ is $\kappa(\mathbf{v}) = \mathbf{v}^T \mathbf{II} \mathbf{v}$, where the symmetric matrix $\mathbf{II}$ is the *second fundamental*

form (which is a special case of the Weingarten matrix, where the first fundamental form is the identity matrix).

The *derivatives of the curvature* are defined by a $2\times2\times2$ tensor with four unique numbers [Rusinkiewicz 2004]:

$$\mathbf{C} = (\partial_{u_1}\mathbf{II}; \partial_{u_2}\mathbf{II}) = \left[\begin{pmatrix} a & b \\ b & c \end{pmatrix}; \begin{pmatrix} b & c \\ c & d \end{pmatrix}\right], \qquad (1)$$

where $\mathbf{u_1}$ and $\mathbf{u_2}$ are the principal directions. Multiplying $\mathbf{C}$ from its three sides by a direction vector $\mathbf{v}$, $\mathbf{C}_{ijk}\mathbf{v}^i\mathbf{v}^j\mathbf{v}^k$ gives a scalar, which is the derivative in the direction $\mathbf{v}$ of the curvature in this direction.

As noted above, we are seeking the loci of the "strongest" inflections, i.e., loci where the curvature derivative is maximal. We therefore define the following.

Definition 3.1 *The* curvature gradient *is the tangent direction of the maximum normal curvature variation. Hence, this direction maximizes the following expression:*

$$\mathbf{g}_p = \arg\max_{\mathbf{v}} \mathbf{C}_{ijk}\mathbf{v}^i\mathbf{v}^j\mathbf{v}^k, \;\; s.t \;\; \|\mathbf{v}\| = 1. \qquad (2)$$

Having defined the curvature gradient direction, we can now proceed to define a demarcating curve point, which is the zero crossing of the normal curvature in the curvature gradient direction.

Definition 3.2 $\mathbf{p}$ *is as a demarcating curve point if the following holds at* $\mathbf{p}$*:* $\kappa(\mathbf{g}_p) = \mathbf{g}_p^T\mathbf{II}\mathbf{g}_p = 0$.

3.2 Computing demarcating curves on meshes

First, for each vertex, the gradient direction is computed, in accordance with Definition 3.1, as well as the value of the curvature in the $\mathbf{g}_p$ direction $\kappa(\mathbf{g}_p) = \mathbf{g}_p^T\mathbf{II}\mathbf{g}_p$. Then, the zero crossings of $\kappa(\mathbf{g}_p)$ on the mesh faces are computed according to Definition 3.2, to create the demarcating curves. We elaborate on these stages below.

Calculation of $\mathbf{g}_p$: To calculate $\mathbf{g}_p$, the second fundamental form $\mathbf{II}$ and the curvature derivative tensor Equation 1 are first found for every vertex [Rusinkiewicz 2004].[1] Then, $\mathbf{g}_p$ can be either computed analytically or estimated numerically (by sampling). Below, we provide the analytic derivation. A slightly different derivation appears in [Mehlum and Tarrou 2006].

To compute $\mathbf{g}_p$ the expression $\mathbf{C}_{ijk}\mathbf{v}^i\mathbf{v}^j\mathbf{v}^k$ is differentiated with respect to $\mathbf{v}$ and compared to zero, as follows. Let $\mathbf{v} = [\cos(\theta), \sin(\theta)]$ be the vector of a unit length, and let a, b, c, d be the coefficients of the curvature derivative tensor (Equation 1). Then, Equation 2 can be written as:

$$\theta_{\mathbf{g}_p} = \arg\max_{\theta}(a\cos^3(\theta) + 3b\cos^2(\theta)\sin(\theta) + \qquad (3)$$
$$+3c\cos(\theta)\sin^2(\theta) + d\sin^3(\theta)).$$

Equation 3 is differentiated with respect to θ and compared to zero. After applying some simple algebraic manipulations, we obtain:

$$3b\cos^3(\theta) + 3(2c-a)\cos^2(\theta)\sin(\theta) + \qquad (4)$$
$$+3(d-2b)\cos(\theta)\sin^2(\theta) - 3c\sin^3(\theta) = 0.$$

Next, the sin term is isolated and the high order cos terms are substituted by $\cos^2(\theta) = 1-\sin^2(\theta)$ to obtain:

$$\cos(\theta) = \sin(\theta)\frac{(a-3c)\sin^2(\theta) + 2c - a}{(3b-d)\sin^2(\theta) - b}. \qquad (5)$$

[1] implemented using the trimesh2 library by S. Rusinkiewicz

After squaring Equation 5 and eliminating $\cos^2(\theta)$, the resulting equation depends only on $\sin(\theta)$:

$$[(-3c+a)^2 + (3b-d)^2]\sin^6(\theta) +$$
$$+[2(2c-a)(-3c+a) - (3b-d)^2 - 2b(3b-d)]\sin^4(\theta) + \qquad (6)$$
$$+[(2c-a)^2 + 2b(3b-d) + b^2]\sin^2(\theta) + -b^2 = 0.$$

This is a third order polynomial in $\sin^2(\theta)$. Therefore, its roots can be found analytically. There can be either one or three real roots, which create two or six extremal angles. If there is a single root, the extremal angle corresponding to the maximum is used to determine $\mathbf{g}_p$. Otherwise, the function in Equation 3 is smoothed with a Gaussian before selecting the global maximum. In this way, close maxima are merged together, giving the larger maximum a bigger weight. Consequently, all the maxima are considered explicitly. In practice, less than 5% of the curve points have two significant roots with a ratio of their values greater than 0.9, and these cases are handled well. The case in which all three maxima have high function values and a demarcating point should be detected (i.e. satisfying Definition 3.2) has not been found in practice.

Calculating demarcating curves: Computing $\mathbf{g}_p$ at every vertex does not suffice for determining the points that satisfy Definition 3.2, since the gradient direction is known only for the vertices and not for all the other points on the mesh. An additional problem is that the direction of the gradient $\mathbf{g}_p$ at every vertex of a mesh face might differ, and thus computing the zero crossing of the curvature along a mesh edge would be inappropriate (as we are looking for zero crossing at a certain direction). Since these problems occur in the calculation of other types of mesh curves, our solution is a variation on [Ohtake et al. 2004; DeCarlo and Rusinkiewicz 2007; Judd et al. 2007] and is briefly described below.

The demarcating curve points are first estimated along the mesh edges. A mesh edge $[\mathbf{p}_1, \mathbf{p}_2]$ contains a demarcating curve point if $\kappa(\mathbf{g}_{p_1})$ and $\kappa(\mathbf{g}_{p_2})$ have opposite signs (i.e., a zero crossing). The exact location of the demarcating curve point is obtained by linear interpolation of the curvature values. Neighboring demarcating curve points are then connected on a face by a straight line to create the demarcating curve itself.

To solve the second problem, faces whose three gradient vectors differ considerably are eliminated from further consideration. (In our implementation, this happen when the angles between the gradients $> \pi/4$.) For faces in which the gradients of only two vertices are similar, the average gradient of the two similar vertices is selected and the curvature of the third vertex is computed in this direction. Obviously, when this gradient is used for the third vertex, it should be rotated so as to coincide with the vertex's tangent plane, as in [Rusinkiewicz 2004; Ohtake et al. 2004]. Now, the zero-crossing interpolation can be applied as described above.

It is important to note that the computation described above is performed offline, prior to interaction with the user. The only operation performed during the actual rendering is the elimination of weak curves. The user provides a *strength parameter*, which is the only parameter that the system requires. This parameter is used as a threshold for the precomputed value of the curvature derivative in the gradient direction ($\mathbf{C}_{ijk}\mathbf{g}_p^i\mathbf{g}_p^j\mathbf{g}_p^k$).

4 Relations to other curves

This section discusses relations between demarcating curves and other well-known curves, in particular valleys and ridges, parabolic lines, zero-mean curvature curves, and suggestive contours.

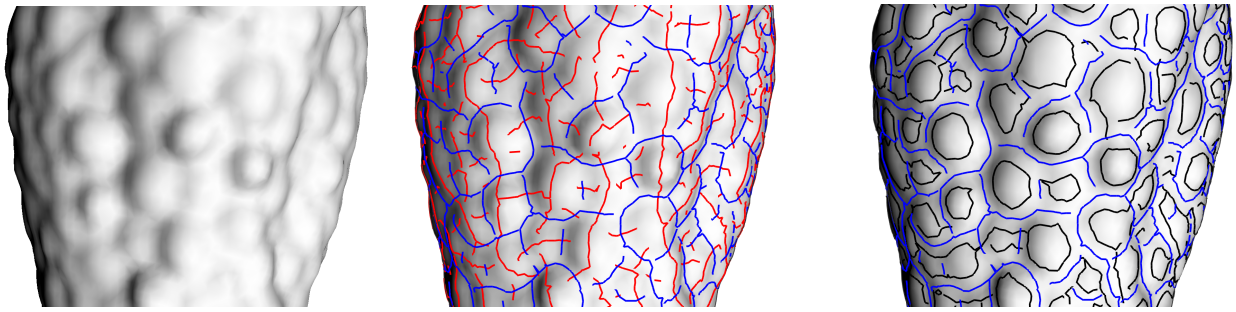

(a) Zoom in of Armadillo's leg (b) Valleys (blue) and ridges (red) (c) Valleys (blue) and demarcating curves (black)

Figure 4: Relation between valleys, ridges, and demarcating curves (on the Armadillo leg). The ridges are not well-defined, the valleys do not bound the bumps, whereas demarcating curves perform much better.

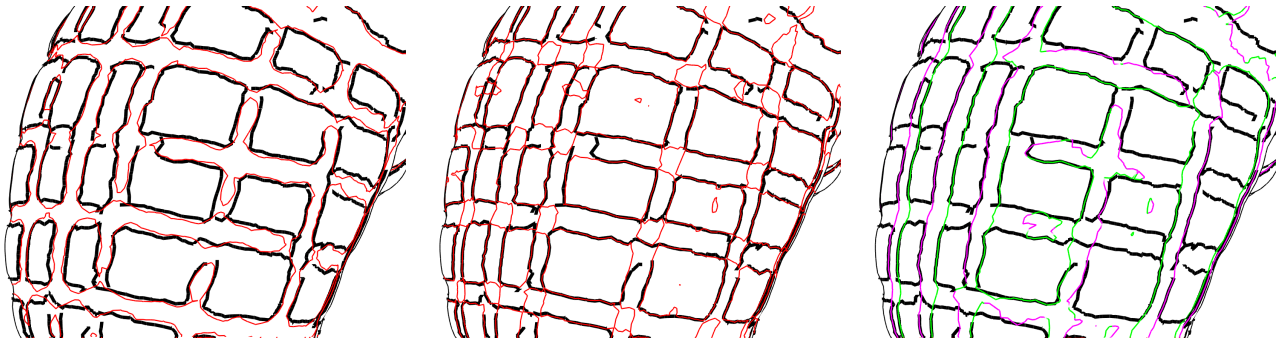

Figure 5: Demarcating curves in black, curves of zero-mean curvature (left) in red, parabolic lines (middle) in red, suggestive contours (right) in green, and suggestive highlights (right) in magenta, on the Armadillo's thigh. The thresholds are all set to zero in order to compare the curves as they are defined. The demarcating curves are closely aligned with the rectangular 3D texture, in contract to the other curves.

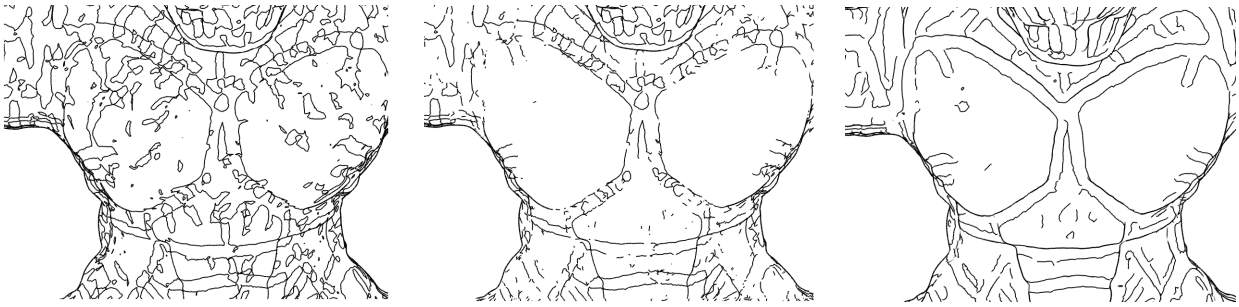

(a) Parabolic lines with different threshold values (b) Demarcating curves

Figure 6: Parabolic lines vs. demarcating curves: zoom into the armadillo's chest

Relation to valleys and ridges: A ridge (valley) point is a point on a manifold, where the positive (negative) principal curvature obtains a maximum (minimum) along its principal direction. Recall that we expect demarcating curves to run between ridges and valleys. Mathematically, this idea can be modeled by locating the curves on a local smooth step edge – a step edge function convolved with a Gaussian (Figure 3). Moreover, demarcating curves run in parallel to ridges and valleys. This is so since in 3D step edges, all normal sections in the $\mathbf{g}_p$ direction are identical, and thus their maxima, minima and zero crossings are equal.

In practice, a demarcating curve will not lie between a valley and a ridge. This is demonstrated in Figure 4, where the ridges fail to capture the round structure of the "bumps" on leg of the Armadillo, yet demarcating curves bound these "bumps" (Figure 4(c)).

Relation to parabolic lines & zero-mean curvature curves: Parabolic (zero-mean curvature) curves are the loci of points with zero Gaussian (mean) curvature. In an ideal surface, where the curves pass through true step edges, zero-mean curvature curves and demarcating curves coincide, since it can be shown that in this case $\mathbf{g}_p$ is a principal direction and both principal curvatures vanish. Moreover, the set of demarcating curve points is a subset of the parabolic curve points, since the Gaussian curvature is zero at demarcating curve points. However, as can be seen in Figure 5 (left & middle), demarcating curves are less sensitive to deviations from the ideal surface.

Figure 6 shows parabolic lines with increasing threshold values of the curvature derivative in the direction orthogonal to the curve. It can be seen that even with no threshold (left) some of the most

important lines do not appear. Moreover, as the threshold increases, some of the "good" lines disappear along with the clutter.

Relation to suggestive contours: Given a viewing direction, let $\mathbf{w}$ be its projection onto the tangent plane. The suggestive contour points are the set of all points on a surface at which the curvature $\kappa(\mathbf{w})$ is zero and the directional derivative of $\kappa(\mathbf{w})$ is positive [DeCarlo et al. 2003].

The set of demarcating curve points is a subset of the union of all the suggestive contour points, viewed from all possible viewing directions. This relationship between the curves simply follows from the fact that they both lie on hyperbolic regions (having negative Gaussian curvature) of the surface. This can also been shown constructively by choosing $w = \mathbf{g}_p$, i.e., the projection of the viewing direction coincides with the gradient direction $\mathbf{g}_p$.

Similarly, it can be shown that the set of demarcating curve points is a subset of the union of all the suggestive highlight points [DeCarlo and Rusinkiewicz 2007].

Figure 5 (right) demonstrates the relations between the curves. It can be seen that many of the suggestive contours (highlights) coincide with the demarcating curves. However, some of the horizontal curves are missing from the suggestive contours (highlights) in this viewpoint. Moreover, when the suggestive highlights appear noisy, demarcating curves usually do not follow.

5 Results and analysis

This section shows results of demarcating curves and compares them to other major curve families. All these curves have only one parameter the user should set. In the examples below, for each of the curves shown, we tried to choose the value that produces the best-looking result for that curve type.

Figure 7 compares different curves drawn on the Armadillo (silhouettes were added to all of them). Apparent ridges and suggestive contours do not convey some important features, especially the circular and rectangular "bumps" on the legs and arms, and the teeth. Suggestive contours are biased towards lines parallel to the viewing plane, and thus lines in certain directions are missed. Apparent ridges may ignore curve points whose normal directions are parallel to the viewing direction, since their employed local maximal curvature tends to be larger near the silhouettes. In this example, valleys better illustrate the 3D structure on the thighs. (Adding ridges degrades the drawing.) Demarcating curves are capable of extracting not only this structure, but also the circular 3D structures on the lower legs.

Figure 8 shows another comparison between the curves. It can be seen that apparent ridges (and similarly suggestive contours, as shown in [Judd et al. 2007]) do not detect the structures on the midsection of the column. Valleys & ridges manage to extract these structures, but fail to accurately detect the curves on the upper section. Demarcating curves better carry the shape structure. Figure 8(d) illustrates how shading can be used to emphasize the demarcating curves – a topic discussed in the next section.

In contrast to valleys & ridges, demarcating curves convey the shape information without resorting to employ different hues. The application of different hues to distinguish between valleys and ridges is somewhat cumbersome [Interrante et al. 1995]. Moreover, valleys & ridges are less effective for detecting closed curves. Finally, as demonstrated in the top section of the column in Figure 8, they do not always convey the structure.

Figure 9 shows an example where the view-dependent curves are more appealing and thus may be considered more pleasing for some non-photorealistic applications. Another limitation of demarcating curves is their inability to highlight protruding or depressing features, which lie at surface curvature extremalities.

Performance evaluation: Demarcating curves are as quick to compute as ridges and valleys and suggestive contours, since they can be computed prior to rendering. Apparent ridges are more expensive to compute since they rely on view-dependent curvature, which needs to be computed for each viewpoint. On a 2.66 GHz Intel Core 2 Duo PC, our unoptimized C++ implementation computed the demarcating curves in 0.15 seconds for 50K polygon meshes and in 1.1 seconds for 500K polygon meshes.

6 Artifact illustration in archaeology

Analysis of archaeological artifacts, such as ceramic vessels, stone tools, coins, seals, figurines etc., is a major source of our knowledge about the past. Traditionally, artifacts are documented and published in 2D photographs, which convey little information about the actual shape (and none about the inner structure) of the objects.

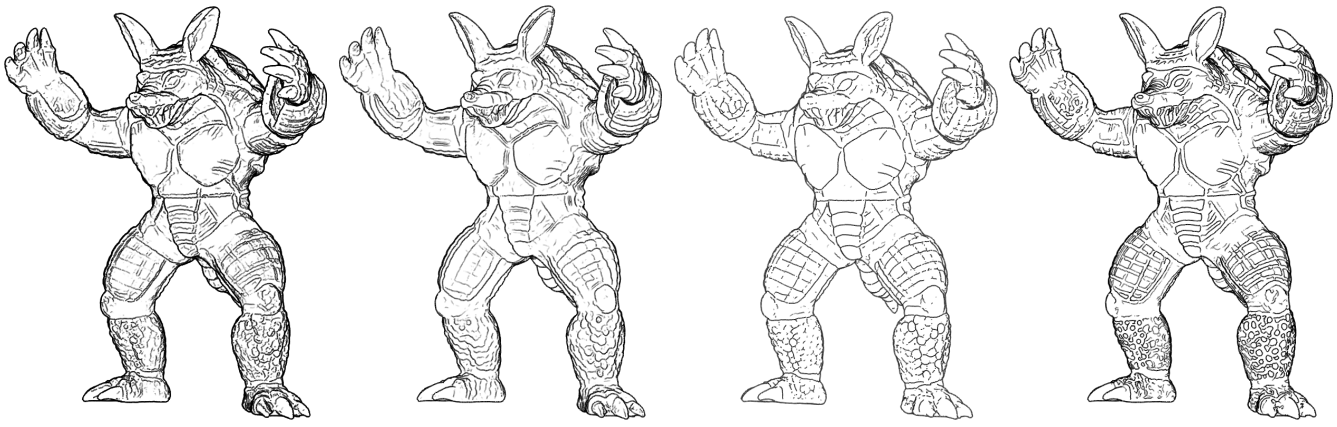

(a) Apparent ridges (b) Suggestive contours (c) Valleys (d) Demarcating curves

Figure 7: Armadillo model. Apparent ridges and suggestive contours do not convey many important features, as can be seen on the upper and lower legs, teeth, and eyes. Even valleys do not convey some of the rectangles on the upper legs and the bumps on the lower legs. Ridges are not shown, since they degrade the drawing. Demarcating curves perform better on this example.

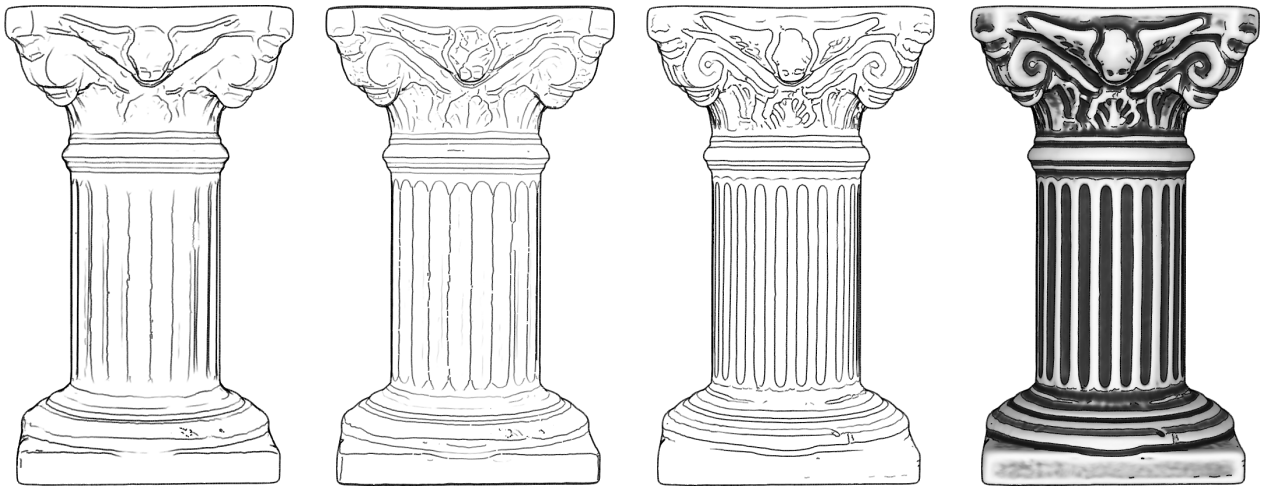

(a) Apparent ridges (b) Valleys & ridges (c) Demarcating curves (d) Shaded demarcating curves

Figure 8: Column model. While lines on the shaft disappear in the apparent ridges drawing and lines on the capital disappear in both apparent ridges and valleys & ridges, they both appear in the demarcating curve drawing.

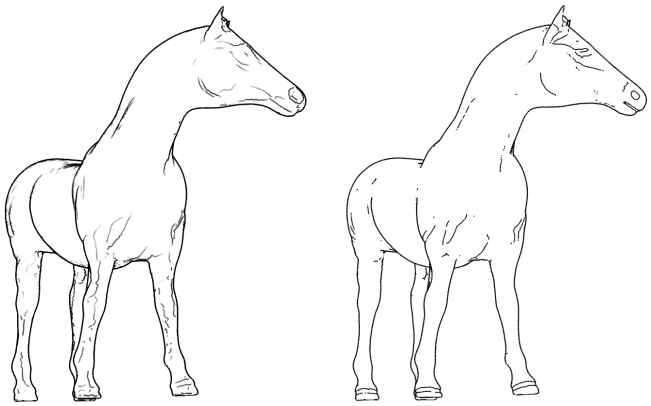

(a) Apparent ridges (b) Demarcating curves

Figure 9: Horse model

The latter properties are described by conventional drawings (Figure 2), which contain sections across the artifacts. These are produced manually – by artists – an extremely time-consuming and expensive procedure, prone to inaccuracies and biases.

Digital archaeological reports are slowly spreading around the globe. When scanned 3D representations replace the 2D ones, accurate, automatic curve drawing will be needed.

Demarcating curves are highly beneficial for models that consist of smooth surfaces overlaid with 3D textures (reliefs). Intuitively, this is so since 3D textures, by their very nature, can be considered locally as "almost images." Therefore, the characteristics of the demarcating curves make them especially appropriate.

The current research is conducted as an interdisciplinary effort with several archaeologists, who defined their needs and evaluated intermediate results. Below we present some results of archaeological relics.

Figure 10 shows a 3D scan of a handle stamped by a Greek official from which it is impossible to read the text. Suggestive, Apparent, and Ridges & Valleys (Figure 11 (a-c)) do not help either. With demarcating curves, we can identify the Greek letters (d). Since the letters are convex and the background is concave, and since demarcating curves demarcate them, it is possible to add a shading scheme to highlight the letters (e-f). It is now possible to read the text as MAPΣΥΆ APTAMITIO, where MAPΣΥΆ[Σ] is the name of an eponym (an official who had the year named after him) and APTAMITIO[Σ] is the name of a month in the Greek (Rhodian) calendar.

Figure 10: A scanned Hellenistic stamped amphora handle from the first century BCE.

The variant shown in Figures 11(e-f) can be generally used for drawing artifacts. Various types of shading schemes can be employed, such as mean-curvature shading [Kindlmann et al. 2003] or exaggerated shading [Rusinkiewicz et al. 2006]. As discussed in Section 4, zero-mean curvature curves and demarcating curves are close to each other. Therefore, using demarcating curves with mean curvature (and often with exaggerated) shading yields eye-pleasing results. The color palette used can vary. Both gray-level shading (Figure 11(e-f)) and the palette suggested by [Gooch et al. 1999] (Figure 1) are shown.

Figure 12 compares mean-curvature shading alone with demarcating curves painted on top of the shaded scanned model of a 65 million year old fossil. It can be noted that the demarcating curves better emphasize the 3D features, yielding crisper images and making them closer to the way archaeological artists portray artifacts.

Figures 13–14 show additional results. Demarcating curves enhance the features that are sometimes difficult to visualize with the

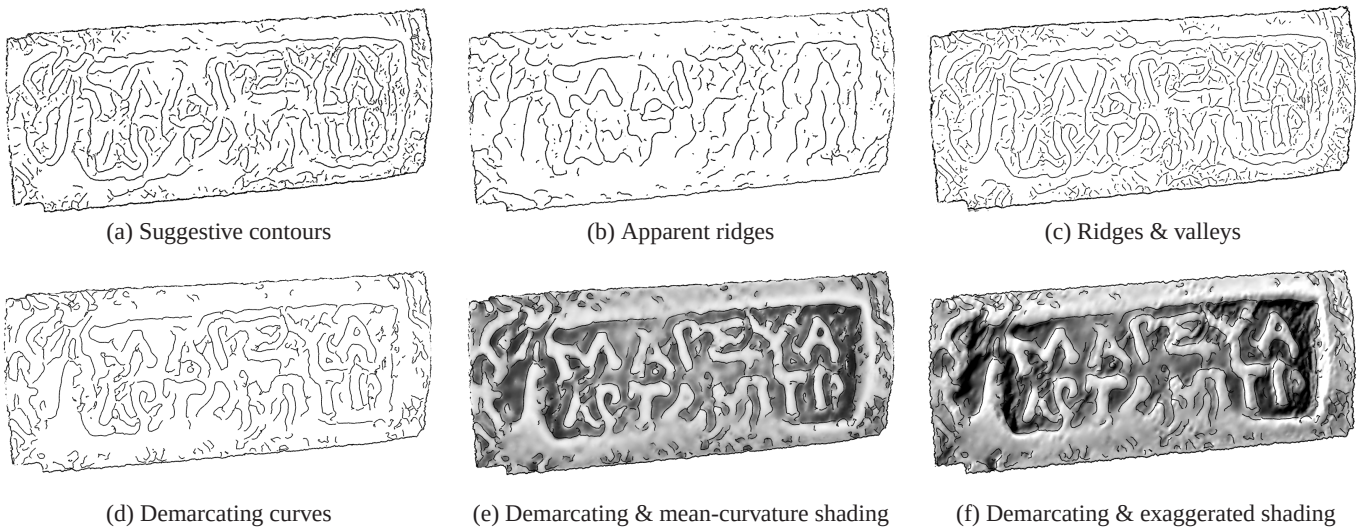

(a) Suggestive contours (b) Apparent ridges (c) Ridges & valleys

(d) Demarcating curves (e) Demarcating & mean-curvature shading (f) Demarcating & exaggerated shading

Figure 11: A Hellenistic stamped amphora handle from the first century BCE. The letters (e.g., Σ) are only visible in (e)-(f)

other curves (and even in the scanned object). Examples include the wings of Cupid, his naval, and the V-shaped decorations in the top Hellenistic lamp; the fine vertical decorations on the bottom Ottoman pipe; and the facial features on the lamp in Figure 14.

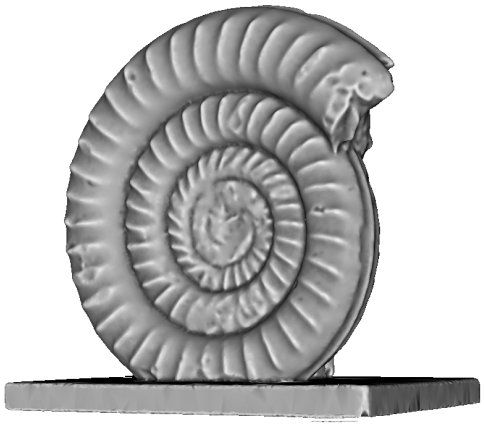

(a) Mean curvature shading

(b) Demarcating curves (with mean curvature shading)

Figure 12: Shading options for an Ammonite fossil

Figures 13(d) & 14(e) illustrate a second variant of drawing, where valleys (or ridges) are used to complement demarcating curves. Here, valley lines are also drawn in gray, in order to portray the concave regions.

The results illustrate the robustness of the algorithm to noise. These archaeological objects are all noisy, not only due to the scanning process but also because of their very nature, found after spending more than 2000 years underground.

To compare the suitability of the different curve types to archaeological illustration, we conducted a preliminary user study. Twenty two professional archaeologists from different universities, attending an international conference on *Computer Applications in the Archaeology of the Levant*, participated in the study. Each person was presented with four pages – each page devoted to a single relic (Figures 1,13,14). Each relic was described by six images: the original scanned object and five different drawings, similarly to Figure 14. (The images with demarcating curves also included valleys in gray.) The order of the five (untitled) drawings changed from page to page. The archaeologists were asked to rank the drawings according to their appropriateness for replacing the traditional manual illustration. Among the four non-shaded line drawings, 71.5% preferred demarcating curves to the other types, 12.5% preferred valleys & ridges and apparent ridges, and 3.5% preferred suggestive contours. In second place valleys & ridges were preferred to apparent ridges (40% vs. 29%). Moreover, 72% preferred the shaded demarcating curves to the non-shaded line drawings.

In an open discussion, the archaeologists indicated that they prefer our drawings to the traditional manual drawings, both aesthetically and because it is also possible to view the drawings interactively in 3D. Manipulation in 3D enables them to see all the important features, as if they held the artifact in their hand. Moreover, they find view-dependent curves less suitable, since the stability of the curves is paramount. These encouraging results suggest that demarcating curves can be a basis for an illustration tool for archaeology.

7 Conclusions

This paper has presented a new class of view-independent curves – *demarcating curves*, defined as the loci of points for which there is a zero crossing of the curvature in the curvature gradient direction.

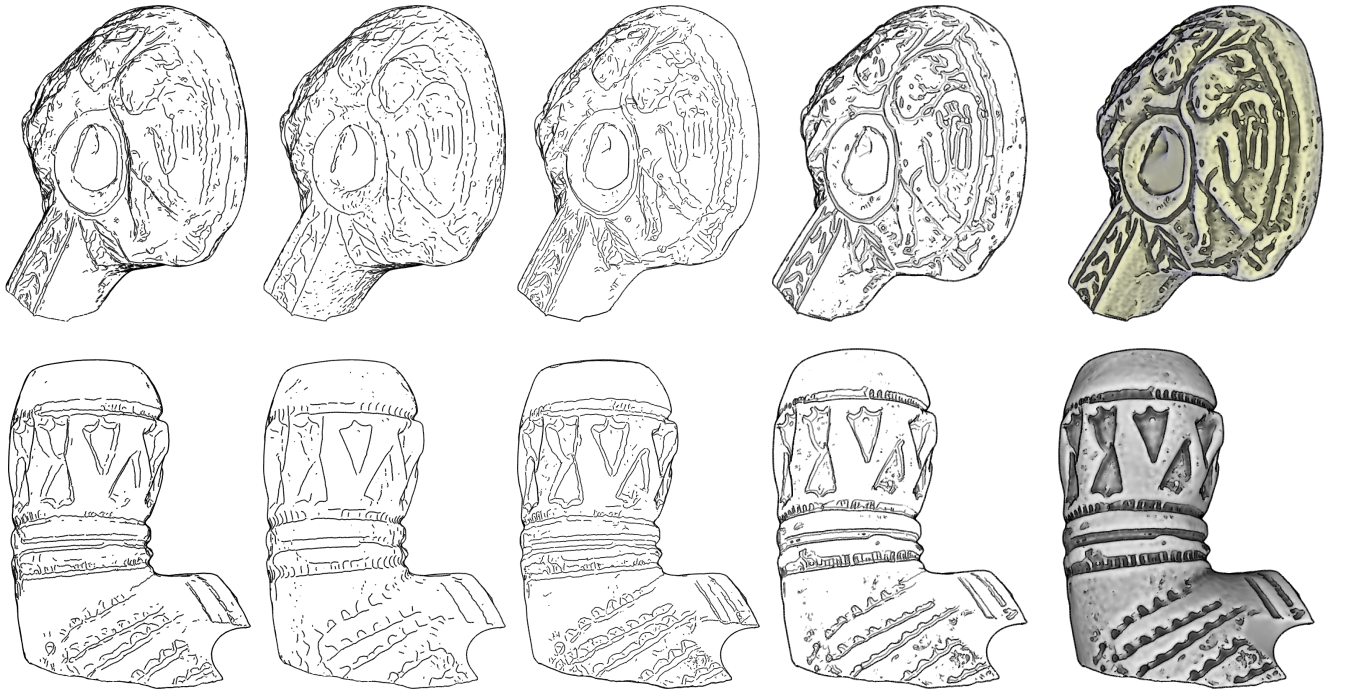

(a) Apparent ridges (b) Suggestive contours (c) Ridges & Valleys (d) Demarcating curves (with gray valleys) (f) Demarcating curves (with mean curvature shading)

Figure 13: Demarcating curves enhance the wings of Cupid, his naval, and the V-shaped decorations on the Hellenistic lamp (top), and the fine vertical decorations on the Ottoman pipe (bottom).

Relations to other types of curves have been discussed.

The utility of the curves for artifact illustration in archaeology has been demonstrated. The results show that demarcating curves effectively capture the 3D information visually. It was welcomed wholeheartedly by the archaeologists.

Since these curves convey meaningful shape information compactly, we intend to utilize them in the future for shape analysis applications, such as similarity based retrieval. In addition, we would like to explore the utility of other types of drawings in archaeology, such as [Deussen et al. 2000].

Acknowledgements: We are grateful to the anonymous referees for their thoughtful comments. This research was supported in part by the Israel Science Foundation (ISF) 628/08, the A.M.N Foundation, and the Joint Technion – Haifa University Research Foundation. We thank Dr. A. Gilboa & Dr. I. Sharon from the Departments of Archaeology at the University of Haifa and the Hebrew University for invaluable discussions and for providing the artifacts and scanning them.

References

BARTESAGHI, A., AND SAPIRO, G. 2001. A system for the generation of curves on 3D brain images. *Human brain mapping 14*, 1, 1–15.

BROWN, B., TOLER-FRANKLIN, C., NEHAB, D., BURNS, M., DOBKIN, D., VLACHOPOULOS, A., DOUMAS, C., RUSINKIEWICZ, S., AND WEYRIC, T. 2008. A system for high-volume acquisition and matching of fresco fragments: Reassembling theran wall paintings. *ACM Trans. Graph. 27*, 3.

COLE, F., GOLOVINSKIY, A., LIMPAECHER, A., BARROS, H., FINKELSTEIN, A., FUNKHOUSER, T., AND RUSINKIEWICZ, S. 2008. Where do people draw lines? *ACM Trans. Graph. 27*, 3.

DECARLO, D., AND RUSINKIEWICZ, S. 2007. Highlight lines for conveying shape. In *NPAR*, 63–70.

DECARLO, D., FINKELSTEIN, A., RUSINKIEWICZ, S., AND SANTELLA, A. 2003. Suggestive contours for conveying shape. *ACM Transactions on Graphics 22*, 3, 848–855.

DECARLO, D., FINKELSTEIN, A., AND RUSINKIEWICZ, S. 2004. Interactive rendering of suggestive contours with temporal coherence. In *NPAR*, 15–24.

DEUSSEN, O., HILLER, S., VAN OVERVELD, C., AND STROTHOTTE, T. 2000. Floating points: A method for computing stipple drawings. *Computer Graphics Forum 19*, 3, 40–51.

DO CARMO, M. P. 1976. *Differential geometry of curves and surfaces*. Prentice-Hall.

GOOCH, B., SLOAN, P. J., GOOCH, A., SHIRLEY, P., AND RIESENFELD, R. F. 1999. Interactive technical illustration. In *Symp. on Interactive 3D Graphics*, 31–38.

HERTZMANN, A., AND ZORIN, D. 2000. Illustrating smooth surfaces. In *ACM SIGGRAPH*, 517–526.

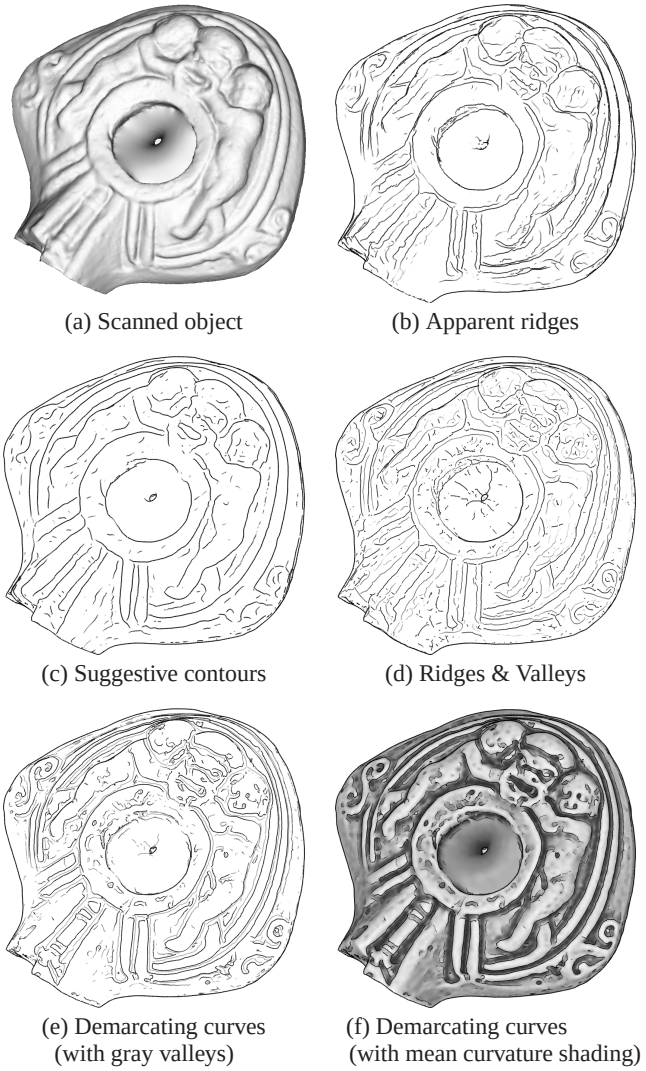

(a) Scanned object (b) Apparent ridges

(c) Suggestive contours (d) Ridges & Valleys

(e) Demarcating curves (with gray valleys) (f) Demarcating curves (with mean curvature shading)

Figure 14: Hellenistic lamp – Note that the small features, such as the facial features, are difficult to visualize even in the scanned object. Demarcating curves make them visible.

INTERRANTE, V., FUCHS, H., AND PIZER, S. 1995. Enhancing transparent skin surfaces with ridge and valley lines. In *IEEE Visualization*, 52–59.

IVERSON, L. A., AND ZUCKER, S. W. 1995. Logical/linear operators for image curves. *IEEE Trans. Pattern Anal. Machine Intell. 17*, 10 (October), 982–996.

JUDD, T., DURAND, F., AND ADELSON, E. 2007. Apparent ridges for line drawing. *ACM Trans. Graph. 26*, 3, 19:1–19:7.

KALNINS, R. D., MARKOSIAN, L., MEIER, B. J., KOWALSKI, M. A., LEE, J. C., DAVIDSON, P. L., WEBB, M., HUGHES, J. F., AND FINKELSTEIN, A. 2002. WYSIWYG NPR: drawing strokes directly on 3D models. In *ACM SIGGRAPH*, 755–762.

KINDLMANN, G., WHITAKER, R., TASDIZEN, T., AND MOLLER, T. 2003. Curvature-Based Transfer Functions for Direct Volume Rendering: Methods and Applications. In *IEEE Vis.*, 67–76.

KOENDERINK, J. J. 1984. What does the occluding contour tell us about solid shape? *Perception 13*, 3, 321–330.

KOENDERINK, J. J. 1990. *Solid shape*. MIT Press.

KOLLER, D., TRIMBLE, J., NAJBJERG, T., GELFAND, N., AND LEVOY, M. 2006. Fragments of the city: Stanford's digital forma urbis romae project. *J. of Roman Arch. 61*, 237–252.

LEE, Y., MARKOSIAN, L., LEE, S., AND HUGHES, J. F. 2007. Line drawings via abstracted shading. *ACM Trans. Graph. 26*, 3, 18:1–18:5.

MAATEN, L. J. P., BOON, P. J., PAIJMANS, J. J., LANGE, A. G., AND POSTMA, E. O. 2006. Computer vision and machine learning for archaeology. In *Computer Applications and Quantitative Methods in Archaeology*, 112–130.

MEHLUM, E., AND TARROU, C. 2006. Invariant smoothness measures for surfaces. *Advances in Comp. Math. 8*, 1-2, 49–63.

OHTAKE, Y., BELYAEV, A., AND SEIDEL, H. P. 2004. Ridge-valley lines on meshes via implicit surface fitting. *ACM Trans. Graph. 23*, 3, 609–612.

PAGE, D., KOSCHAN, A., ABIDI, M., AND OVERHIOLT, J. 2006. Ridge-valley path planning for 3D terrains. In *IEEE Int. Conf. on Robotics and Automation*, 119–124.

PAULY, M., KEISER, R., AND GROSS. 2003. Multi-scale feature extraction on point-sampled surfaces. *Computer Graphics Forum 22*, 3, 281–290.

PEARSON, D. E., AND ROBINSON, J. A. 1985. Visual communication at very low data rates. *Proceedings of IEEE 73*, 795–812.

PENNEC, X., AYACHE, N., AND THIRION, J. 2000. Landmark-based registration using features identified through differential geometry. In *Handbook of Medical Imaging*. 499–513.

RUSHMEIER, H. 2005. Eternal Egypt: experiences and research directions. In *Modeling and Visualization of Cultural Heritage*, 22–27.

RUSINKIEWICZ, S., BURNS, M., AND DECARLO, D. 2006. Exaggerated shading for depicting shape and detail. *ACM Transactions on Graphics (Proc. SIGGRAPH) 25*, 3 (July).

RUSINKIEWICZ, S. 2004. Estimating curvatures and their derivatives on triangle meshes. In *Proc. 3D Data Processing, Visualization and Transmission*, 486–493.

SAITO, T., AND TAKAHASHI, T. 1990. Comprehensible rendering of 3D shapes. In *ACM SIGGRAPH*, 197–206.

STERN, E. 1995. *Excavations at Dor*. Jerusalem: Institute of Archaeology of the Hebrew University.

STROTHOTTE, T., AND SCHLECHTWEG, S. 2002. *Non-Photorealistic Computer Graphics*. Morgan Kaufmann.

STYLIANOU, G., AND FARIN, G. 2004. Crest lines for surface segmentation and flattening. *IEEE Trans. on Visualization and Computer Graphics 10*, 5, 536–544.

XIE, X., HE, Y., TIAN, F., AND SEAH, H.-S. 2007. An effective illustrative visualization framework based on photic extremum lines (PELs). *IEEE Trans. on Visualization and Computer Graphics 13*, 6, 1328–1335.

YOSHIZAWA, S., BELYAEV, A., AND SEIDEL, H. P. 2005. Fast and robust detection of crest lines on meshes. In *ACM Symposium on Solid and Physical Modeling*, 227–232.